Scientia Iranica C (2017) 24(6), 3064–3073

Sharif University of Technology
Scientia Iranica
Transactions C: Chemistry and Chemical Engineering
www.scientiairanica.com

H_2S removal using ZnO/SBA-3: New synthesis route and optimization of process parameters

A. Vahid[a,*], M. Qandalee[b] and S. Baniyaghoob[c]

a. *Research Institute of Petroleum Industry, Tehran, Iran.*
b. *Department of Basic Science, Garmsar Branch, Islamic Azad University, Garmsar, Iran.*
c. *Department of Chemistry, Faculty of Basic Science, Islamic Azad University, Science and Research Branch, Hesarak, Tehran, Iran.*

Received 21 December 2016; received in revised form 4 July 2017; accepted 21 October 2017

KEYWORDS
Air pollution;
H_2S;
Mesoporous materials;
Removal;
Zinc oxide.

Abstract. H_2S is a major toxic compound that could be found in air, water, and fossil fuels and causes some bad effects such as acidic rain and corrosion. In the present work, SBA-3 (Santa Barbara University no. 3) with three different weight percentages of ZnO, namely, 5%, 10%, and 15%, was synthesized via an in situ approach. All synthesized samples were characterized using atomic absorption spectrometry, X-Ray Diffraction (XRD), nitrogen adsorption, and Transmission Electron Microscopy (TEM). The obtained results from XRD and nitrogen adsorption confirmed that all the samples almost retained their ordered structure after incorporation of ZnO nanoparticles within the mesopores of SBA-3. TEM images showed that ZnO nanoparticles were arranged along the direction of mesopores of SBA-3. Then, adsorption of H_2S from a model gas was investigated. A three-factor Box-Behnken design with five center points and one response was performed for the evaluation of effect of three process parameters, namely, ZnO wt%, space velocity, and temperature, on the adsorption of H_2S and a quadratic model (r^2 : 0.9185) was developed to navigate the design space. Temperature had the largest and space velocity had the lowest effect on the breakthrough of H_2S. The optimum breakthrough time (t_{bp}) was 588 min.

1. Introduction

Ordered mesoporous silica materials are formed from the silica-coated micelles of a surfactant template via sol-gel process. They have attracted much attention in various areas since their discovery [1,2]. Due to their unique properties, notably large surface area and pore size, tunable pore size, chemical functionalization of pore wall, and high thermal stability [3-5], mesoporous silica materials have attracted great attention in many fields such as catalysis [6], environmental purification [7-9], air pollution [10-13], and desulfurization [14]. It has been noted that the principal feature of the mesoporous silica materials, namely, their periodic and ordered mesoporous structure, does not offer specific advantages in some special applications, as it occurs in catalysis, e.g. by acid catalyst [4,6]. To overcome this problem, synthesis of mesoporous materials with proper active phases has been the goal of alternative ways [6].

There are many synthetic strategies for the in situ or post-synthesis functionalization of mesoporous materials by metallic nanoparticles. In the former case,

*. *Corresponding author. Tel./Fax: +98 21 48255042*
E-mail addresses: avahid753@gmail.com (A. Vahid); qandalee@gmail.com (M. Qandalee); baniyaghoob@gmail.com (S. Baniyaghoob)

doi: 10.24200/sci.2017.4573

the most usual method is doping of reaction mélange with metal salts [15]. In post-synthetic approach, the most common synthesis routes are: I) incipient wetness impregnation [16]; II) ion exchange [17]; III) equilibrium adsorption [18]; IV) metal complex immobilization [19]; V) vapor phase deposition [20]; and VI) sonication [21-24]. One of the interesting applications of mesoporous materials is adsorption of hazardous gases. Among them, hydrogen sulfide, H_2S (g), is a common gaseous pollutant, which is colorless, odorous, and highly toxic [25-30]. Furthermore, during the combustion of fossil fuels, sulfur-containing compounds such as H_2S, thiols, and thiophene derivatives convert to SO_x. It means that H_2S has remarkable contribution to the amount of emitted SO_x into the environment. Subsequently, emitted SO_x reacts with water vapor and causes formation of acid rain, which is harmful to mammals and other living organisms [31-33]. Removal of H_2S from a gas stream could be done by several methods, namely, adsorption onto a solid adsorbent, absorption using a liquid solution, and catalytic oxidation [34-38]. Adsorption by metal oxide sorbents is recognized as an energy-efficient technology for H_2S removal. The adsorption capacity of adsorbent depends on the nature of the adsorbent, e.g. functional groups present, specific surface area, and pore size distribution; the nature of adsorbate, e.g. molecular weight and size, solubility, and pK_a or pK_b for weak acids or bases; and solution conditions, e.g. pH, temperature, and adsorbate concentration [39-42]. One of the appropriate methods for the preparation of such sorbent is embedding of proper metal oxides such as ZnO (active part) on silicate mesoporous materials [43-46]. Three-dimensional mesoporous materials are good candidates for this goal [47-51]. SBA-3 has a peculiar bimodal pore system, same as SBA-15, but can be synthesized in two hours instead of two days [52]. It is well known that bimodal three-dimensional arrangement of a mesoporous material improves mass transfer of guest species [53,54]. In this work, ZnO nanoparticles were incorporated within the mesopores of SBA-3 via an in situ approach. After that, adsorption of H_2S using ZnO/SBA-3 samples was investigated and the effect of important process parameters was evaluated using RSM methodology.

2. Experimental

2.1. Synthesis

All chemical compounds were purchased from Merck and were used as received. The general procedure for synthesis of SBA-3 was reported [45-48]. In this work, zinc-containing SBA-3 was synthesized via an in situ approach with some modifications [32]. In a typical synthesis, 3 grams of cetyltrimethylammonium bromide (CTAB) and 150 mL of water were mixed to yield a clear solution. Predetermined amount of $Zn(acac)_2$, about 0.054 g for 5 wt.%, was added to the micellar solution. After 10 minutes of stirring, the hydrophobic $Zn(acac)_2$ was dissolved within the core of CTAB micelles, which had hydrophobic nature, and the solution became clear. After that, 50 mL of HCl (37%) and, then, 15 mL of Tetraethyl orthosilicate (TEOS) were added to yield a light yellow suspension. The suspension was stirred for two hours, filtered, washed with sufficient amounts of water and acetone, and dried in oven at 100°C over night. Four samples were synthesized and denoted by Zny/SBA, in which y represents the weight ratio of Zn/SBA in the corresponding sample. Thermocalcination of as-synthesized SBA-3 was carried out under flow of air up to 550°C for 6 hours.

2.2. Characterization

X-Ray Diffraction (XRD) patterns were recorded on a Seifert TT 3000 diffractometer using nickel filtered Cu Kα radiation of wavelength 1.5405 Å. Nitrogen adsorption was measured at 77 K using a BEL-SORP-mini porosimeter. Prior to analysis, the samples were outgassed in-vacuo for 4 h at 463 K until a vacuum of 0.1 Pa was firmly reached. Determination of H_2S was carried out via argenometry.

2.3. H_2S removal

The concentration of H_2S in the feed model (helium) was 5000 ppm. This concentration was taken as the criterion for the H_2S breakthrough during adsorption of H_2S. Adsorption measurements for H_2S were performed using a lab made apparatus. Scheme 1 displays the lab-made adsorption apparatus used in this study.

H_2S at outlet was adsorbed in the caustic solution and analyzed via UOP-209 standard test method. In brief, the caustic solution was added to isopropyl alcohol containing a small amount of ammonium hydroxide. The solution was titrated potentiometrically with alcoholic silver nitrate solution of known concentration using a combined electrode consisting of glass reference and silver-silver sulfide indicating electrode.

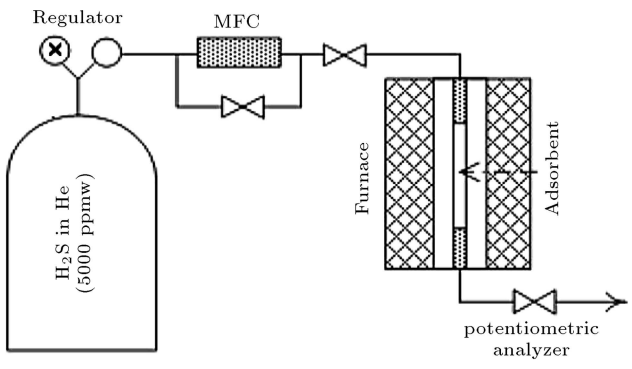

Scheme 1. Schematic representation of the lab-made apparatus used for removal of H_2S.

2.4. Experimental design

Box-Behnken Design (BBD) is a class of rotatable or nearly rotatable second-order designs based on three-level incomplete factorial designs. A three-process-factor design (A: *temperature* (°C), B: *space velocity* (h^{-1}), C: *ZnO* (wt%)) was used for the investigation of the main effects and their interaction with H_2S adsorption of synthesized samples. BBD was combined with response surface modeling and quadratic programming.

Coding of actual variables (X_i) was carried out as follows:

$$\chi_i = \frac{X_i - \frac{(X_{high}+X_{low})}{2}}{\frac{(X_{high}-X_{low})}{2}}, \quad (1)$$

where χ_i is the dimensionless coded value of the ith factor, X_i the uncoded value of the ith independent variable, and X_{high} and X_{low} the high and low levels of uncoded factors, respectively. The ranges of all the three independent variables are given in Table 1.

The effect of variables and interactions on the adsorption process was explained by the following quadratic polynomial equation, which contained independent variables, quadratic interactions, and squared terms:

$$y = \beta_0 + \sum_{i=1}^{3} \beta_i \chi_i + \sum_{i=1}^{3} \beta_{ii} \chi_i^2 + \sum_{i=1}^{3} \sum_{i<1}^{3} \beta_{ij} \chi_i \chi_j + \varepsilon, \quad (2)$$

where y is predicted response of adsorption breakthrough (t_{bp}), χ_i and χ_j the coded factors, β_0 intercept, β_i linear coefficient, β_{ij} quadratic coefficient, β_{ii} squared coefficient, i and j the index numbers for variables, and ε the random error, which shows different sources of variability.

3. Results and discussion

The concentration of zinc in the SBA-3 was determined by atomic absorption spectrometry via classic wet chemistry method. The results indicated that at least 95 wt% of zinc was incorporated into the mesopores of SBA-3.

In the synthesis method, $Zn(acac)_2$ is a hydrophobic complex; thus, after addition to the CTAB solution, it diffuses to the hydrophobic core of CTAB micelles and dissolves in its core, which results in a clear solution. On the other hand, before addition of CTAB, the complex dose not dissolve; it creates a suspension and

Table 1. Factors and levels for the BBD design.

Factors		Level		
		−1	0	+1
A	Temperature (°C)	25	187.5	350
B	Space velocity (h^{-1})	2000	5000	8000
C	ZnO (wt%)	5	10	15

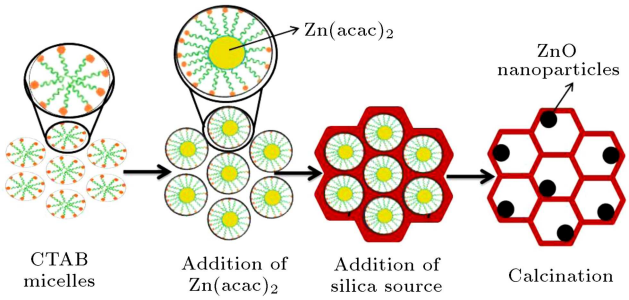

Scheme 2. Proposed mechanism for synthesis of ZnO/SBA3.

settles down. After addition of silica source, $Zn(acac)_2$ complex is surrounded by the silica wall. Finally, during calcination, organic part of zinc complex is fully burned and it converts to ZnO nanoparticles. In this mechanism, size of ZnO NPs is controlled by the size of mesopores. The proposed mechanism of synthesis is schematically illustrated in Scheme 2.

3.1. XRD

XRD is one of the best methods for the investigation of structure of ordered porous materials. Figure 1(a)-(d) shows the evolution of the low-angle XRD patterns with increase in zinc content in calcined samples. In all the samples, XRD pattern includes a strong diffraction peak, which is characteristic of mesoporous materials prepared through surfactant-templated procedure. This strong peak is usually referred to as the d_{100} reflection when a hexagonal lattice is present in the corresponding sample. Higher order diffraction peaks are also observable, of which number and intensity are qualitative measures of higher structural order in the

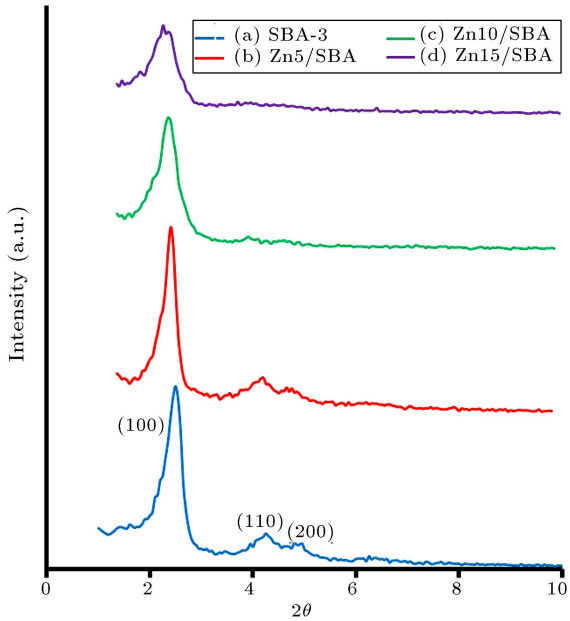

Figure 1. XRD patterns of (a) SBA-3, (b) Zn5/SBA, (c) Zn10/SBA, and (d) Zn15/SBA.

corresponding sample. By comparing the Zny/SBA (Figure 1(b)-(d)) with the corresponding parent SBA-3 (Figure 1(a)), it can be observed that increase in zinc content results in an increase in the broadness of the d_{100} reflection along with a slight shift to lower diffraction angles. It can be deduced that increase in zinc content within the SBA-3 results in disordering of CTAB cylindrical micelles. Subsequently, this leads to the loss of structural order of synthesized SBA-3. However, the obtained results indicated that up to 15 wt% of zinc content had no significant effect on the structural order of SBA-3. Two other signals could be indexed to the (200) and (210) reflections of the typical hexagonal cell. Their observation constituted a clear probe of the existence of a high structural order in the mesopore system. However, these two signals became very weak and broad after incorporation of zinc within SBA-3, which could be associated with the loss of structural order of corresponding sample. As the amount of zinc increases, the structural order of mesopore system decreases.

3.2. Nitrogen adsorption and TEM

In addition to the expected mesoporous system, the hexagonal pore array characteristic of the SBA-3 material can be appreciated through nitrogen adsorption measurements. Nitrogen sorption of all the samples exhibits type IV isotherm according to IOPAC nomenclature (Figure 2(a)-(d)).

Sharpness of the capillary condensation step decreases as the amount of ZnO increases. However, a slight increase in the mean pore diameter can be seen due to the swallowing of CTAB micelles by $Zn(acac)_2$. Textural properties of all samples were calculated via geometrical (pressure-independent) method and are given in Table 2 [50].

As can be seen in Table 2, as the loading of zinc increases, pore volume of all the samples decreases while pore diameter increases. According to this observation, it can be suggested that most of zinc nanoparticles are incorporated within the mesopore architecture.

TEM is a powerful technique for direct observation of the pore architecture of porous materials. TEM images of SBA-3 and Zn15/SBA are illustrated in Figure 3(a)-(c), respectively. The hexagonal structure is clearly visible in both samples, indicating that

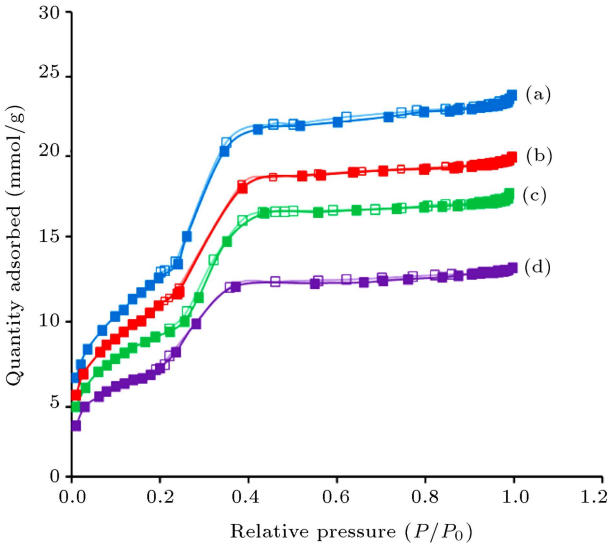

Figure 2. Nitrogen adsorption isotherms of (a) SBA-3, (b) Zn5/SBA, (c) Zn10/SBA, and (d) Zn15/SBA.

structural order is still presents in the SBA-3 support after 15 wt% of metal loading. The presence of ZnO nanoparticles is more visible in Figure 3(c).

For evaluation of the in situ incorporation of ZnO within SBA-3 in terms of accessibility of active sites (ZnO) to adsorption of H_2S, a well-known wet impregnation of SBA-3 with aqueous $Zn(NO_3)_2$ solution following the usual protocols was performed. Then, a typical H_2S adsorption test at 10 wt% Zn/SiO_2, 300°C, and *gas hourly space velocity* of 5000 h^{-1} was carried out. Interestingly, t_{bp} of in situ prepared Zn10/SBA was higher (19%) than that of impregnated Zn10/SBA. This result can be attributed to the well dispersion as well as more accessibility of active sites (ZnO nanoparticles) in the former adsorbent.

The reaction of ZnO with H_2S is as follows:

$$ZnO + H_2S \rightarrow ZnS + H_2O.$$

H_2S at outlet was adsorbed in the caustic solution and analyzed via UOP-209 standard test method. In brief, the caustic solution was added to isopropyl alcohol containing a small amount of ammonium hydroxide. The solution was titrated potentiometrically with alcoholic silver nitrate solution of known concentration using a combined electrode including glass reference and silver-silver sulfide indicating electrode.

Table 2. Textural properties of Zn/SBA samples containing different weight percentages of ZnO (0, 5, 10, and 15).

Sample name	a_0 (nm)	S_{BET} (m^2 g^{-1})	Pore size (nm)	Total pore volume (cm^3 g^{-1})	Pore wall thickness (nm)
SBA-3	3.2	833	2.03	1.41	1.018
Zn5/ SBA	3.32	716	2.14	1.36	1.022
Zn10/ SBA	3.41	634	2.21	1.24	1.038
Zn15/ SBA	3.58	502	2.31	1.11	1.10

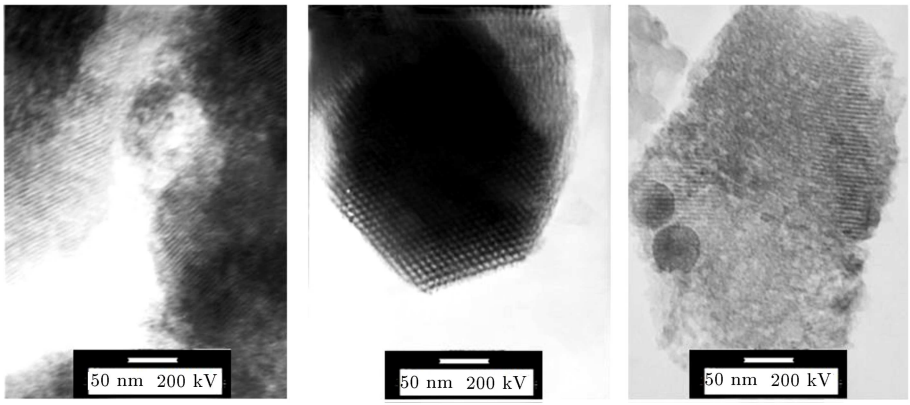

Figure 3. TEM images of (a) SBA-3 and (b) Zn15/SBA. Scale bar represents 50 nm.

3.3. Statistical analysis

As obtained from BBD method with three main factors and 5 times of replication in center point, 17 runs were designed and the obtained results are given in Table 3. t_{bh} for bare SBA-3 at 25°C and *gas hourly space velocity* of 5000 h^{-1} was found to be 36 minutes.

However, adsorption of H_2S on bare SBA-3 at higher temperature was negligible because chemisorption did not take place as a result of absence of ZnO active site. Furthermore, at higher temperatures, i.e. 187 and 300°C, physisorption did not occur [24,25].

Sequential model sum of square, lack of fit test, and model summary statistics were utilized to decide on the adequate model for explanation of adsorption process parameters. Model summary statistics showed that quadratic model was better for further analysis of obtained results, because it had maximum "adjusted R-squared" and the "predicted R-squared" values; also, it had p value lower than 0.01. Data are given in Table 4.

Table 3. The design matrix and experimental data of t_{bp} from the BBD design.

St. run order	Run	A[a]	B[b]	C[c]	t_{bp} (min)
3	1	25	2000	10	92
12	2	350	2000	10	370
4	3	25	8000	10	85
13	4	350	8000	10	265
11	5	25	5000	5	99
8	6	350	5000	5	220
1	7	25	5000	15	109
9	8	350	5000	15	541
15	9	187.5	2000	5	150
7	10	187.5	8000	5	175
16	11	187.5	2000	15	360
17	12	187.5	8000	15	239
6	13	187.5	5000	10	170
5	14	187.5	5000	10	190
10	15	187.5	5000	10	188
14	16	187.5	5000	10	193
2	17	187.5	5000	10	163

[a]Temperature (°C); [b]Space velocity (h^{-1}); [c]ZnO (wt%).

The ANOVA (analysis of variance) table is given in Table 5. Among three quadratic terms, two quadratic terms, i.e. A^2 and B^2, were not significant and, therefore, they were omitted from the model; thus, the model was refitted to the data again. After that, the only significant quadratic term was C^2. As can be deduced from ANOVA table and the statistical F-test, all the three factors are statistically significant. As a general rule, the term which has a higher F has larger effect on the response. Among three main factors, temperature has the largest effect on t_{bp} and increases it; however, space velocity has the lowest effect on t_{bp}. Among three interactions, AC has the largest effect on t_{bp} while AB has the lowest one. The obtained quadratic model is statistically significant and can explain the relation between the factors and their interaction with t_{bp}. The lack of fit term of model is also significant. This means that the data are well fitted to the model and can explain the behavior of the system during adsorption process.

The regression equation obtained after ANOVA in terms of actual factors is as follows:

$$\begin{aligned} t_{bp} = &+ 131.40705 + (0.072051 * \text{Temp.}) \\ &+ (0.025090 \times \text{S.V.}) - (27.41731 \times \text{ZnO}) \\ &- \left(5.02564E^{-005} \times Temp. \times \text{S.V.}\right) \\ &+ (0.095692 \times \text{Temp.} \times \text{ZnO}) \\ &- \left(2.43333E^{-003} \times \text{S.V.} \times \text{ZnO}\right) + 1.83833 \\ &\times \text{ZnO}^2. \end{aligned} \quad (3)$$

Figure 4(a)-(c) illustrate the 3D graph of interactions

Table 4. Adequacy of the model.

Source	Std. dev.	R-squared	Adjusted R-squared	Predicted R-squared	PRESS
Linear	58.50001934	0.80086756	0.754914	0.607674	87651.64
2FI	35.46692743	0.94369671	0.909915	0.812613	41865.09
Quadratic	18.06753205	0.9897722	0.976622	0.882805	26183.13
Cubic	13.40522286	0.99678268	0.987131		+

Table 5. Analysis of variance of the response surface model for the prediction of t_{bp}.

Source	Sum of squares	Degree of freedom	Mean square	F value	p value Prob > F	Remark
Model	2.20E+05	7	31397.45	77.77	< 0.0001	Significant
A-temp.	1.28E+05	1	1.28E+05	316.48	< 0.0001	Significant
B-S.V.	5408	1	5408	13.4	0.0052	Significant
C-ZnO	45753.13	1	45753.13	113.33	< 0.0001	Significant
AB	2401	1	2401	5.95	0.0374	Significant
AC	24180.25	1	24180.25	59.9	< 0.0001	Significant
BC	5329	1	5329	13.2	0.0055	Significant
C^2	8945.65	1	8945.65	22.16	0.0011	Significant
Residual	3633.37	9	403.71	—	—	Significant
Lack of fit	2914.57	5	582.91	3.24	0.1386	—
Pure error	718.8	4	179.7	—	—	Not significant
Cor total	2.23E+05	16	—	—	—	

of three main effects, i.e. AB, AC, and BC, on t_{bp}. As can be seen, AC interaction has the largest effect on t_{bp} and AB has the lowest effect. AB interaction is between these two interactions. In Figure 4(a), at lowest temperature, t_{bp} does not change with increase in space velocity. However, increase in t_{bp} is observable with the evolution of temperature; its reaches the maximum value at 350°C. This increase is almost linear and no curvature can be seen. This might be due to the change in the type of adsorption of H_2S at different temperatures. At low temperatures, the main process is physisorption and as the temperature increases, chemisorption becomes the predominant process. Figure 4(b) (AC) shows the similar behavior of AB. At low temperatures, increase in ZnO content has no considerable effect on t_{bp}. But, as the temperature increases, the effect of ZnO content becomes very important. It can be suggested that ZnO is activated at high temperature, which results in higher t_{bp}. Effect of BC is displayed in Figure 4(c). Decrease in space velocity causes increase in t_{bp}. However, at high ZnO content, this phenomenon is more noticeable. In comparison with the recent studies, the effect of space velocity is low in this study. This could be due to the three-dimensional and bimodal pore structure of SBA-3, which leads to less constrained diffusion of guest molecules into the pores in comparison with the two-dimensional unimodal pore system of other mesoporous materials such as MCM-41 [42-44]. When there is low diffusion limitation, the effect of temperature becomes predominant, even with respect to ZnO content. An experimental run was also carried out at optimum condition, i.e. ZnO = 15 wt%, Temp. = 350°C, and space velocity = 2000 h^{-1}. The obtained t_{bp} was 588 min.

4. Conclusion

In this work, an in situ approach was used to incorporate ZnO nanoparticles into the mesopores of SBA-3. In the reported method, a hydrophobic complex, i.e. $Zn(acac)_2$, was used as metal precursor. This hydrophobic complex diffuses into the hydrophobic core of CTAB micelles (template) and is then surrounded by hydrolyzed silicate species during synthesis. After calcination, $Zn(acac)_2$ converts to ZnO nanoparticles, the size of which is smaller than the size of mesopores of the SBA-3. The obtained results from XRD, TEM, and nitrogen adsorption revealed that zinc containing samples retained their well-ordered structure after incorporation of ZnO up to 15 wt%. Adsorption of H_2S using the synthesized samples was carried out and effect of process parameters was investigated using response surface methodology via Box-Behnken design.

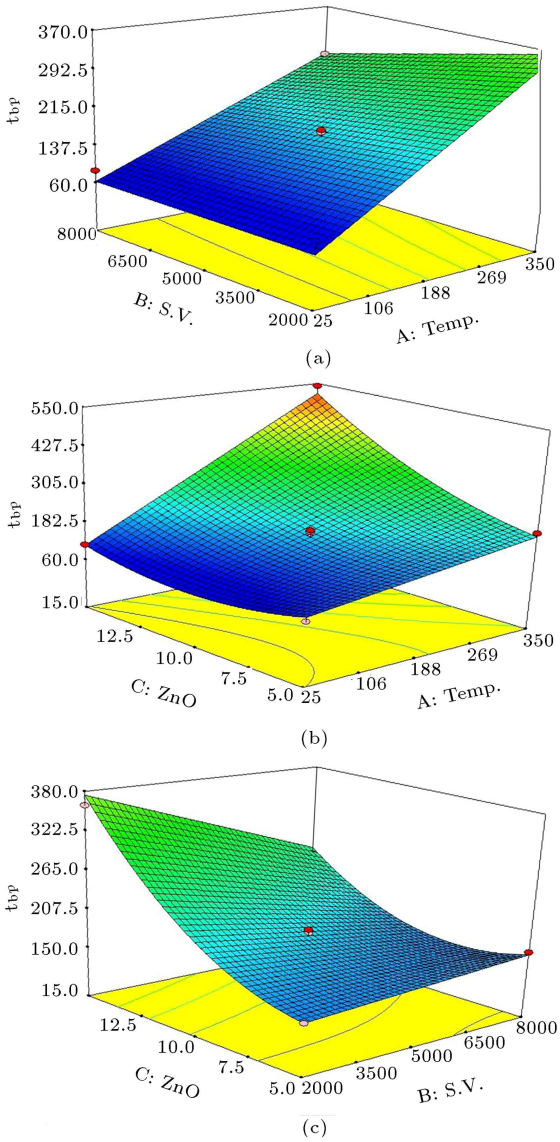

Figure 4. 3D plots describing the response surface t_{bp} in minute as a function of (a) temperature versus space velocity (ZnO = 10 wt%), (b) temperature versus ZnO (space velocity: 5000 h^{-1}), and (c) space velocity vs. ZnO (temperature = 187.5).

Among three factors, i.e. temperature, ZnO wt%, and gas hourly space velocity, the latter had the highest effect and temperature had the lowest effect on t_{bp}. According to the obtained results from adsorption of H_2S, it can be inferred that method of synthesis results in well dispersion and well accessibility of ZnO embedded in the SBA-3 and it can be used as good adsorbent for removal of H_2S.

Acknowledgment

This work was financially supported by Iran National Science Foundation (INSF) under the research project number of 90007451.

References

1. Kresge, C.T., Leonowicz, M.E., Roth, W.J., Vartuli, J.C. and Beck, J.S. "Ordered mesoporous molecular sieves synthesized by a liquid-crystal template mechanism", *Nature*, **359**, pp. 710-712 (1992).
2. Wei, J., Sun, Z., Luo, W., Li, Y., Elzatahry, A.A., Al-Enizi, A.M., Deng, Y. and Zhao, D. "New insight into the synthesis of large-pore ordered mesoporous materials", *J. Am. Chem. Soc.*, **139**(5), pp. 1706-1713 (2017).
3. Beck, J.S., Vartuli, J.C., Roth, W.J., Leonowicz, M.E., Kresge, C.T., Schmitt, K.D., Chu, C.T.W., Olson, D.H., Sheppard, E.W., McCullen, S.B., Higgins, J.B. and Schlenker, J.L. "A new family of mesoporous molecular sieves prepared with liquid crystal templates", *Journal of American Chemical Society*, **114**, pp. 10834-10846 (1992).
4. Deng, X., Chen, K. and Tüysüz, H. "Protocol for the nanocasting method: Preparation of ordered mesoporous metal oxides", *Chem. Mater.*, **29**(1), pp. 40-52 (2017).
5. Wan, Y. and Zhao, D.Y. "On the controllable soft-templating approach to mesoporous silicates", *Chemical Reviews*, **107**, pp. 2821-2860 (2007).
6. Taguchi, A. and Schuth, F. "Ordered mesoporous materials in catalysis", *Microporous and Mesoporous Materials*, **77**, pp. 1-45 (2005).
7. Mathieua, Y., Soularda, M., Patarina, J. and Molière, M. "Mesoporous materials for the removal of SO_2 from gas streams", *Fuel Processing Technology*, **99**, pp. 35-42 (2012).
8. Gibson, L.T. "Mesosilica materials and organic pollutant adsorption: part A removal from air", *Chemical Society Reviews*, **43**, pp. 5163-5172 (2014).
9. Moritz, M. and Geszke-Moritz, M. "Application of nanoporous silicas as adsorbents for chlorinated aromatic compounds. A comparative study", *Mater Science & Engineering C, Mater for Biological Application.*, **41**, pp. 42-51 (2014).
10. Chew T.L., Ahmad, A.L. and Bhatia, S. "Ordered mesoporous silica (OMS) as an adsorbent and membrane for separation of carbon dioxide (CO_2)", *Advances in Colloid Interface Science*, **153**, pp. 43-57 (2010).
11. Inada, M., Enomoto, N. and Hojo, J. "Fabrication and structural analysis of mesoporous silica-titania for environmental purification", *Microporous and Mesoporous Materials*, **182**, pp. 173-177 (2013).
12. Gibson, L.T. "Mesosilica materials and organic pollutant adsorption: part B removal from aqueous solution", *Chemical Society Reviews*, **43**, pp. 5173-5182 (2014).
13. Mathieua, Y., Tzanisa, L., Soularda, M., Patarina, J., Vierlingb, M. and Molière, M. "Adsorption of SOx by oxide materials: A review", *Fuel Processing Technology*, **114**, pp. 81-100 (2013).

14. Stanislaus, A., Marafi, A. and Rana, M.S. "Recent advances in the science and technology of ultra low sulfur diesel (ULSD) production", *Catalysis Today*, **153**, pp. 1-68 (2010).

15. Bronstein, L., Emer, E.K., Berton, B., Burger, C., Erster, S.F. and Antonietti, M. "Successive use of amphiphilic block copolymers as nanoreactors and templates: preparation of porous silica with metal nanoparticles", *Chemistry of Materials*, **11**, pp. 1402-1405 (1999)

16. Yuranov, I., Moeckli, P., Buffat, S.E., Kiwi-Minsker, P. and Renken, L. "Pd/SiO_2 catalysts: synthesis of Pd nanoparticles with the controlled size in mesoporous silicas", *Journal of Molecular Catalysis A: Chemical*, **192**, pp. 239-251 (2003).

17. Chen, H., Matsumoto, A., Nishimiya, N. and Tsutsumi, K. "A novel ion exchange method to modify mesoporpous molecular sieve Al-FSM-16 by cobalt-complex", *Chemistry Letters*, **9**, pp. 993-994 (1999).

18. Zhang, W.H., SHI, J.L., Wang, L.Z. and Yan, D.S. "Preparation and characterization of ZnO clusters inside mesoporous silica", *Chemistry of Materials*, **12**, pp. 1408-1413 (2000)

19. Zhang, L., Sun, T. and Ying, J.Y. "Oxidation catalysis over functionalized metalloporphyrins fixated within ultralarge-pore transition metal-doped silicate supports", *Chemical Communication*, pp. 1103-1105 (1999).

20. Zhang, Y., Lam, F.L.-Y., Hu, X., Yan, Z. and Sheng P.J. "Fabrication of copper nanowire encapsulated in the pore channels of SBA-15 by metal organic chemical vapor deposition", *Journal of Physical Chemistry C*, **111**, pp. 12536-12541 (2007).

21. Grass, M.E., Yue, Y., Habas, S.E., Rioux, R.M., Teall, C.I., Yang, P. and Somorjai, G.A. "Silver ion mediated shape control of platinum nanoparticles: removal of silver by selective etching leads to increased catalytic activity", *Journal of Physical Chemistry C*, **112**, pp. 4797-4804 (2008).

22. Li, L., Shi, J.-L., Zhang, L.-X., Xiong, L.-M. and Yan, J.-N. "A novel and simple in-situ reduction route for the synthesis of an ultra-thin metal nanocoating in the channels of mesoporous silica materials", *Advance Materials*, **16**, pp. 1079-1082 (2004).

23. Fryxell, G.E. "The synthesis of functional mesoporous materials", *Inorganic Chemical Communication*, **9**, pp. 1141-1150 (2006).

24. Wang, Z.-J., Xie, Y. and Liu, C.-J. "Synthesis and characterization of noble metal (Pd, Pt, Au, Ag) nanostructured materials confined in the channels of mesoporous SBA-15", *Journal of Physical Chemistry C*, **112**, pp. 19818-19824 (2008).

25. Husein, M.M., Patruyo, L., Pereira-Almao, P. and Nassar, N.N. "Scavenging H_2S(g) sorption from oil phases by means of ultradispersed sorbents", *Journal of Colloid and Interface Science*, **342**, pp. 253-260 (2010).

26. Nassar, N.N., Husein, M.M. and Pereira-Almao, P. "Ultradispersed particles in heavy oil: Part II, sorption of H_2S (g)", *Fuel Processing Technology*, **91**, pp. 169-174 (2010).

27. Zhanga, J., Liua, M., Zhanga, R., Wanga, B. and Huang, Z. "Insight into the properties of stoichiometric, reduced and sulfurized CuO surfaces: Structure sensitivity for H2S adsorption and dissociation", *Molecular Catalysis*, **438**, pp. 130-142 (2017).

28. Rowan, F.E., Docherty, N.G., Coffey, J.C. and O'Connell, P.R. "Sulphate-reducing bacteria and hydrogen sulphide in the aetiology of ulcerative colitis", *The British Journal of Surgery*, **96**, pp. 151-158 (2009).

29. Dorman, D.C., Moulin, F.J.-M., Mcmanus, B.E., Mahle, K.C., James, R.A. and Struve, M.F. "Cytochrome oxidase inhibition induced by acute hydrogen sulfide inhalation: correlation with tissue sulfide concentrations in the rat brain, liver, lung, and nasal epithelium", *Toxicological Sciences*, **65**, pp. 18-25 (2002).

30. Hua, L., Dub, Y. and Long, Y. "Relationship between H_2S emissions and the migration of sulfur-containing compounds in landfill sites", *Ecological Engineering*, **106**, pp. 17-23 (2017).

31. Hogan. M.C., Monosson, E. and Cleveland, C. "Abiotic factor. Encyclopedia of earth", *National Council for Science and the Environment*, Washington DC (2010)

32. Samadi-Maybodi, A., Teymouri, M., Vahid, A. and Miranbeigi, A. "In situ incorporation of nickel nanoparticles into the mesopores of MCM-41 by manipulation of solvent-solute interaction and its activity toward adsorptive desulfurization of gas oil", *Journal of Hazardous Materials*, **192**, pp. 1667-1676 (2011).

33. Srivastav, A. and Srivastava, V.C. "Adsorptive desulfurization by activated alumina", *Journal of Hazardous Materials*, **170**, pp. 1133-1140 (2009).

34. Feng, Y., Li, Y., Wang, J., Wu, M., Fan, H. and Mi, J. "Insights to the microwave effect in the preparation of sorbent for H_2S removal: Desulfurization kinetics and characterization", *Fuel*, **203**, pp. 233-243 (2017).

35. Wang, J., Qiu, B., Han, L., Feng, G., Hu, Y., Chang, L. and Bao, W. "Effect of precursor and preparation method on manganese based activated carbon sorbents for removing H_2S from hot coal gas", *Journal of Hazardous Materials*, **213**, pp. 184-192 (2012).

36. de Morais Batista, A.H., de Sousa, F.F., Honorato, S.B., Ayala, A.P., Filho, J.M., de Sousa, F.W., Pinheiro, A.N., de Araujo, J.C.S., Nascimento, R.F., Valentini, A. and Oliveira, A.C. "Ethylbenzene to chemicals: Catalytic conversion of ethylbenzene into styrene over metal-containing MCM-41", *Journal of Molecular Catalysis A: Chemical*, **315**, pp. 86-98 (2010).

37. Sahu, R., Song, B.J., Im, J.S., Jeon, Y. and Lee, C.W. "A review of recent advances in catalytic hydrocracking of heavy residues", *Journal of Industrial and Engineering Chemistry*, **27**, pp. 12-24 (2015).

38. Untea, I., Dancila, M., Vasile, E. and Belcu, M. "Structural, morphological and textural modifications of ZnO-TiO_2 HTGD based sorbents induced by Al_2O_3 addition, thermal treatment and sulfurizing process", *Powder Technology*, **191**, pp. 27-33 (2009).

39. Chytil, S., Kure, M., Lodeng, R. and Blekkan, E.A. "On the initial deactivation of MnxOy-Al_2O_3 sorbents for high temperature removal of H_2S from producer gas", *Fuel Processing Technology*, **133**, pp. 183-194 (2015).

40. Duman, O. and Tunc, S. "Electrokinetic properties of vermiculite and expanded vermiculite: Effects of pH, clay concentration and mono- and multivalent electrolytes", *Separation Science and Technology*, **43**, pp. 3755-3776 (2008).

41. Barbaa, D., Cammarotab, F., Vaianoa, V., Salzanoc, E. and Palmaa, V. "Experimental and numerical analysis of the oxidative decomposition of H_2S", *Fuel*, **198**, pp. 68-75 (2017).

42. Duman, O. and Ayranci, E. "Adsorptive removal of cationic surfactants from aqueous solutions onto high-area activated carbon cloth monitored by in situ UV spectroscopy", *Journal of Hazardous Materials*, **174**, pp. 359-367 (2010).

43. Subrenat, A., Le Leuch, L.M. and Le Cloirec, P. "Electrodeposition of copper and iron oxides on to activated carbon fibre cloths: application to H_2S and NH_3 removal from air", *Environmental Technology*, **29**, pp. 993-1000 (2008).

44. Bagreev, A., Menendez, J.A., Dukhno, I., Tarasenko, Y. and Bandosz, T.J. "Bituminous coal-based activated carbons modified with nitrogen as adsorbents of hydrogen sulfide", *Carbon*, **42**, pp. 469-476 (2004).

45. Polychronopoulou, K., Fierro, J.L.G. and Efstathiou, A.M. "Novel Zn-Ti-based mixed metal oxides for low-temperature adsorption of H_2S from industrial gas streams", *Applied Catalysis B: Environmental*, **57**, pp. 125-137 (2005).

46. Hazrati, N., Abdouss, M., Vahid, A., Miran Beigi, A.A. and Mohammadalizadeh, A. "Removal of H_2S from crude oil via stripping followed by adsorption using ZnO/MCM-41 and optimization of parameters", *International Journal of Environmental Science and Technology*, **11**, pp. 997-1006 (2014).

47. Miran Beigi, A.A., Hazrati, N., Abdouss, M. and Vahid, A. "Solvent selection in impregnation of zinc oxide nanoparticles into MCM-41 investigation of its ability toward H_2S removal from crude oil", *Journal of Nanoanalysis*, **1**, pp. 41-46 (2014).

48. Abdouss, M., Hazrati, N., Miran Beigi, A.A., Vahid, A. and Mohammadalizadeh, A. "Effect of the structure of the support and the aminosilane type on the adsorption of H_2S from model gas", *RSC Advances*, **4**, pp. 6337-6345 (2014).

49. Martínez, M.L., Ponte, M.V., Beltramone, A.R. and Anunziata, O.A. "Synthesis of ordered mesoporous SBA-3 materials using silica gel as silica source", *Materials Letters*, **134**, pp. 95-98 (2014).

50. Chen, F., Xu, X.J., Shen, S., Kawi, and S. and Hidajat, K. "Microporosity of SBA-3 mesoporous molecular sieves", *Microporous and Mesoporous Materials*, **75**, pp. 231-235 (2004).

51. Anunziata, O.A., Martínez, M.L. and Costa, M.G. "Characterization and acidic properties of Al-SBA-3 mesoporous material", *Materials Letters*, **64**, pp. 545-548 (2010).

52. Martíneza, M.L., Gostaa, M.B., Montib, G.A. and Anunziata, O.A. "Synthesis, characterization and catalytic activity of AlSBA-3 mesoporous catalyst having variable silicon-to-aluminum ratios", *Microporous and Mesoporous Materials*, **144**, pp. 183-190 (2011).

53. Haskouri, J.E, Dallali, L., Fernandez, L., Garro, N., Jaziri, S., Latorre, J., Guillem, C., Beltran, A., Beltran, D. and Amoros, P. "ZnO nanoparticles embedded in SBA-3-like mesoporous silica materials: Synthesis and characterization", *Physica E*, **42**, pp. 25-31 (2009).

54. Kruk, M. and Jaroniec, M. "Characterization of the Porous Structure of SBA-15", *Chemistry of Materials*, **12**, pp. 1961-1968 (2000).

Biographies

Amir Vahid received his BS degree in Applied Chemistry from Razi University, Kermanshah, Iran, in 2002, and then MS and PhD degrees both in Analytical Chemistry from University of Mazandaran in 2006 and 2011, respectively. He is now Assistant Professor at Research Institute of Petroleum Industry and works on crude oil characterization and upgrading. His scientific field of interest includes analytical chemistry, spectroscopy, oscillating chemical reactions, catalysis, adsorption; petroleum chemistry, environmental pollution, and synthesis and characterization of organic and inorganic porous materials and their application in oil and gas industry in lab, bench, and pilot scales.

Mohammad Qandalee was born in 1978 in Iran. He received his PhD degree from University of Mazandaran in 2010 under the supervision of Professor Asghari. In 2006, he moved to the Garmsar Islamic

Azad University as Assistant Professor and in 2017, he went to the University of Burgos, Spain, as a Visiting Researcher under the supervision of Professor Tomas Torroba Perez. His research interest focuses on synthetic organic chemistry, heterocyclic chemistry, and synthesis of chemiluminescence active sensors.

Sahar Baniyaghoob received her BS degree in Pure Chemistry from Tehran University in 2003, MS and PhD degrees in Inorganic Chemistry from Sharif University of Technology, Tehran, Iran, in 2005 and 2010, respectively. She is currently Assistant Professor at Science and Research Branch, Islamic Azad University, Tehran, Iran. She is working in the field of inorganic chemistry with special interest in the investigation of the interactions between Schiff base complexes, free radicals, metal catalyzed reactions, and synthesis of biologically important molecules and macromolecules using UV-Vis spectroscopy. Furthermore, she uses the knowledge of chemistry in oil industry, especially for applying useful techniques for desulfurization and upgrading of heavy oils.